The three-dimensional Ising model and its Fisher analysis: A paradigm of liquid-vapor coexistence in nuclear multifragmentation

C. M. Mader and A. Chappars*
Hope College, Holland, Michigan 49423, USA

J. B. Elliott, L. G. Moretto, L. Phair, and G. J. Wozniak
Nuclear Science Division, Lawrence Berkeley National Laboratory, Berkeley, California 94720, USA
(Received 13 March 2001; revised manuscript received 11 March 2003; published 1 December 2003)

Recent analysis of multifragmentation data in terms of Fisher's droplet model has led to the extraction of the nuclear liquid-vapor phase diagram. A similar analysis of Coniglio-Klein clusters of the $d=3$ Ising model shows an equivalently good Fisher's scaling which can be used to obtain the Ising phase diagram, thus supporting the claim of the nuclear multifragmentation analysis in terms of a phase transition.

DOI: 10.1103/PhysRevC.68.064601 PACS number(s): 25.70.Pq, 24.10.Pa, 24.60.Ky, 64.60.Ak

Nuclear multifragmentation is a process occurring at the limits of nuclear excitation, and, as such, portrays a deep richness and complexity. While the fundamental problem of dynamics vs statistics is still debated, it appears ever more clearly that many thermal/statistical features underlie the empirical body of data. In particular, two features associated with the fragment multiplicities are found to be quite pervasive in all multifragmentation reactions. They have been named "reducibility" and "thermal scaling" [1–4].

Reducibility is the property that the probability of observing n fragments of a given size is expressible in terms of an elementary one-fragment probability. This property indicates that the fragments are created independently from one another. Both binomial, and its limiting form, Poissonian reducibilities have been extensively documented experimentally for nuclear multifragmentation [1–4].

Thermal scaling is the linear dependence of the logarithm of the one-fragment probability with $1/T$, most directly observed in an Arrhenius plot. It indicates that the emission probability for a fragment of type i has a Boltzmann dependence

$$p_i = p_0 e^{-B_i/T}, \tag{1}$$

where B_i is a "barrier" corresponding to the production process.

The combination of these two empirical features powerfully attests to a statistical mechanism of multifragmentation in general, and to liquid-vapor coexistence specifically [4].

Both features are found in the Fisher's droplet model [5–8] which describes the vapor clusterization in equilibrium with its liquid. An analysis in terms of Fisher's droplet model has been performed recently on several sets of nuclear multifragmentation data [4,9,10]. A remarkable agreement with this model has been observed, and the corresponding liquid-vapor phase diagram has been extracted [9,10]. These conclusions are still the subject of some debate [11] and the work presented in this paper continues that debate.

Many statistical models have been proposed as an explanation for multifragmentation. It is our intention to identify a model which, while as simple as possible, still captures the essential features observed in the experiments. Percolation in its many varieties has been widely used [12–15]. However, while being simple, it does not lend itself to a nontrivial thermal study [16]. The three-dimensional Ising model satisfies both the criteria of simplicity in its Hamiltonian and lends itself to a thermal treatment with nontrivial results.

While the Ising model has been widely studied in terms of its continuous phase transition [17–26] and, in the guise of the lattice gas, has even been used to study nuclear systems [27–37], the problem of clusterization has received relatively little attention.

We will show that this model contains both the features of reducibility and thermal scaling observed in nuclear multifragmentation. In showing the features of thermal scaling we will demonstrate that for temperatures below the critical temperature, the slopes of the Arrhenius plots associated with the individual sizes of the clusters, or the barriers, portray a dependence on the cluster size A of the form $B \propto A^{\sigma}$, where σ is a critical exponent which relates the size to the cluster surface. In addition, the individual Arrhenius plots for each cluster size can be absorbed into a single scaling function identical to that of Fisher's droplet model [5–8], which defines the liquid-vapor coexistence line up to the critical temperature.

The Hamiltonian of the Ising model has two terms: the interaction between nearest-neighbor (nn) spins in a fixed lattice and the interaction between the fixed spins and an external applied field H_{ext}:

$$H = -J \sum_{i,j=\{nn\}} s_i s_j - H_{ext} \sum_i s_i, \tag{2}$$

where J is the strength of the spin-spin interaction. In the absence of an external magnetic field, the system exhibits a first-order phase transition for temperatures up to the critical point at which it exhibits a continuous phase transition. The critical temperature for the three-dimensional Ising model has not been determined analytically; how-

*Present address: Marietta College, Marietta, OH 45750.

ever, high temperature expansion techniques have yielded a value of $T_c = 4.511\,52 \pm 0.000\,04\ J/k_B$ [38].

The zero-field Ising model is isomorphous with the lattice gas model [39,40]. The positive spins are mapped to unoccupied sites in a lattice gas and the negative spins are mapped to occupied sites. The phase transition is then analogous to a liquid-vapor phase transition. If a correspondence is observed between features of the Ising model and nuclear multifragmentation, it could strengthen the case for nuclear multifragmentation being the signature for a liquid-gas phase transition of excited nuclei.

In the present study, the calculations were performed via a code using standard Monte Carlo techniques [41]. For each lattice configuration, a random initial configuration of spins and a temperature were selected. Thermalization was reached via the Swendsen-Wang cluster spin-flip algorithm [23] using the Hoshen-Kopelman algorithm for cluster identification. After the system was thermalized, "geometric" clusters, i.e., nearest-neighbor-like spins, were identified (also using the Hoshen-Kopelman algorithm) and then the Coniglio-Klein algorithm [19] was used to break the geometric clusters into "physical" clusters. The code was tested against the published results both in Ref. [41] and in other literature. Since we are interested in studying liquid-vapor coexistence, all calculations are performed at zero external field ($H_{ext}=0$). The lattice contains 50^3 spins, and periodic boundary conditions are used to minimize finite size effects. The use of the Swendsen-Wang algorithm and Coniglio-Klein clusters gives us hope that the clusters analyzed in this work are most closely related to the physical clusters observed in fluids and do not suffer from problems such as the percolating critical point reached away from the thermal critical point or the presence of the Kertész line [13,21].

Our intent in this paper is not to study large (or not so large) Ising lattices to increase the already vast accumulation of large lattice Ising simulation papers. Rather it is to show that like the experimental nuclear multifragmentation yields, the Ising model contains reducibility and thermal scaling and (approximately) obeys the scaling inherent in the Fisher droplet model (which also contains reducibility and thermal scaling). To do this we chose a reasonably large lattice with periodic boundary conditions to free ourselves (as much as possible) from the complicating effects of finite size, but not so large a lattice that computation time would be prohibitive.

We now proceed to analyze the cluster yields in the same way as has been done with nuclear multifragmentation data [1–4]. We shall consider first whether the multiplicity distributions for individual clusters manifest Poissonian reducibility. Figure 1 shows the multiplicity distributions for a sample of cluster sizes and temperatures. The solid lines represent Poisson distributions calculated from the corresponding mean multiplicities. The distributions are nearly Poissonian not only for the cases shown, but for all sizes and all temperatures. Poissonian reducibility is empirically verified in the Ising model.

This signifies that the probability of finding m clusters of size A depends only on the probability of finding one cluster of that size and is nearly independent of the probability of finding clusters of any other size. This feature is also observed in percolation models and nuclear fragmentation [4].

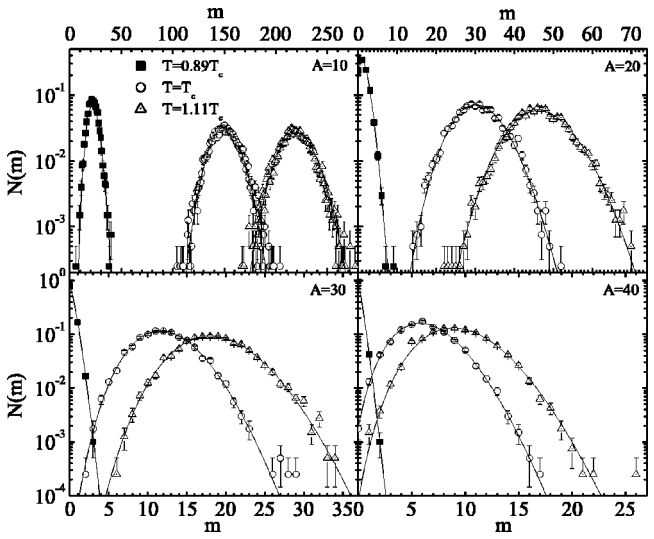

FIG. 1. The probability distributions for obtaining m clusters of size A at the three temperatures indicated. The solid lines are Poisson distributions with means given by the Monte Carlo data.

If the cluster distributions exhibit thermal scaling, the distributions must be of the form given in Eq. (1). Thus in an Arrhenius plot [a semilog graph of the number of clusters of size A (n_A) vs $1/T$], the distributions should be linear.

As shown in Fig. 2, this is indeed the case over a wide range of temperatures ($0<T<T_c$) and cluster sizes. While we have shown distributions for clusters up to size $A=100$, the trend continues for larger clusters, but with poorer statistics. This linearity extends over more than four orders of

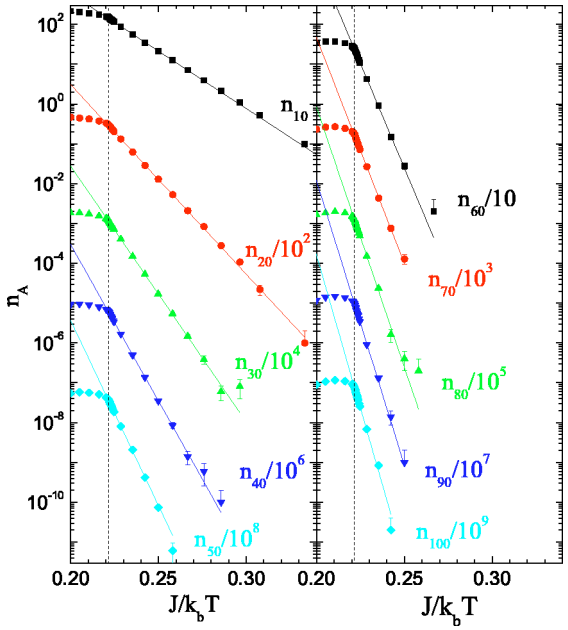

FIG. 2. (Color online) Arrhenius plots of the cluster distributions. A statistical error bar is shown when it exceeds the size of the data point. The lines are fits of the form given in Eq. (1). The critical temperature is indicated by the dashed line.

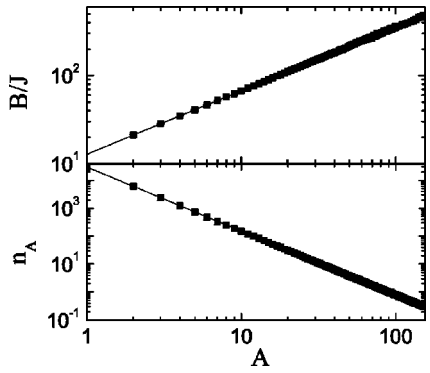

FIG. 3. The upper panel shows the extracted "barriers" from the fits to the cluster distributions. The line is a fit of the form given in Eq. (3). The lower panel shows the power law behavior of the cluster distribution at $k_BT/J=4.515$. The line is a fit of the form given in Eq. (6). In both panels, error bars are smaller than the data point.

magnitude. This behavior is consistent with the form of Eq. (1) and the changing slopes of the Arrhenius plots indicate that the independent thermal formation of clusters is controlled by a dominant size-dependent barrier. This feature has been amply verified in nuclear multifragmentation [1–4]. By fitting the linear regions of the cluster distributions below the critical temperature, the barriers can be extracted. The barriers for each cluster size are shown in Fig. 3.

These barriers find their origin in the number of broken bonds associated with a cluster which should be proportional to the surface area of the cluster itself. Therefore for large enough A, they should be well described by a power law:

$$B(A) = c_0 A^{\sigma}, \tag{3}$$

with $\sigma \simeq 2/3$. The extracted barriers obey the relationship $B=(12.77\pm0.04)JA^{(0.723\pm0.008)}$. The fit is shown in Fig. 3. Errors are only those returned from the fitting procedure. An estimate of the systematic errors is given below.

The value for σ determined from the barriers is close to 2/3, the value one would expect for spherical clusters of closely packed spherical objects [22]. Previous studies have determined σ from scaling relations between critical exponents based on Fisher's droplet model and suggest a value of $\sigma \sim 0.64$ [5,6,18,22]. Duflot *et al.* used a cluster method to determine σ for an Ising model [36] and obtained values that are consistent with those found in this study.

This picture leads naturally to the interpretation of c_0 as a surface energy coefficient. The value of c_0 obtained above is in good agreement with other estimates of the surface energy coefficient based on the analysis of the nucleation rate in the $d=3$ Ising model [42] and suggests that the clusters are approximately cubical in shape. The surface tension in the $d=3$ Ising model is $2J$ so that the surface energy coefficient of cubical clusters would then be $12J$.

As mentioned above, the features of reducibility and thermal scaling discussed above can be found united in Fisher's droplet model for the cluster abundance in a vapor as a function of cluster size and temperature. The formula is

$$n_A(T) = q_0 A^{-\tau} \exp\left(\frac{A\Delta\mu}{T}\right)\exp\left(-\frac{c_0 A^{\sigma}\varepsilon}{T}\right), \tag{4}$$

where q_0 is a normalization constant, τ is a topological critical exponent, $\Delta\mu$ is the difference in chemical potential of the system and the liquid, c_0 is the surface energy coefficient, and $\varepsilon=(T_c-T)/T_c$. The formula is valid for temperatures up to the critical point, at which point the surface free energy of a cluster ($c_0A^{\sigma}\varepsilon$) vanishes. The parametrization used in Fisher's droplet model is only one example of a more general form of the scaling assumption $n_A=A^{-\tau}f(X)$ and $X=A^{\sigma}\varepsilon^{\phi}$ where $f(X)$ is some general scaling function which: is valid on both sides of the critical point; will vary, for small X ($T\sim T_c$ and small A) and $\varepsilon>0$, as $\exp(-X)$ with $\sigma=1/(\beta\delta)=1/(\gamma+\beta)\sim 0.64$ for three-dimensional Ising systems, 8/15 for two-dimensional Ising systems, or ~ 0.45 for three-dimensional percolation systems and $\phi=1$; and will vary, for large X (T far from T_c or large A) and $\varepsilon>0$, as $\exp(-X)$ with $\sigma=(d-1)/d$ for all d-dimensional systems and with $\phi=2\nu$, where $\nu\sim 0.63$ for three-dimensional Ising systems, $\nu=1$ for two-dimensional Ising systems, and $\nu\sim 0.88$ for three-dimensional percolation lattices. However, this more general scaling function $f(X)$ does not lend itself as easily to a physical interpretation as does the parametrization given by Fisher's droplet model and it is this physical interpretation which is important to the application of this method to the nuclear data.

Fisher's droplet model contains thermal scaling up to T_c and the dependence of the barrier on the cluster size through the critical exponent σ [5,6]. Working at coexistence, so $\Delta\mu=0$, we rewrite Eq. (4) and group the temperature dependent terms giving

$$n_A(T) = q_0 A^{-\tau} \exp\left(\frac{c_0 A^{\sigma}}{T_c}\right)\exp\left(-\frac{c_0 A^{\sigma}}{T}\right) = B_0 \exp\left(\frac{-B(A)}{T}\right). \tag{5}$$

It is apparent that Fisher's droplet model exhibits reducibility. The distribution in droplet (cluster) size is Poissonian by construction: each component of droplet size A is an ideal gas without the canonical constraint of overall constituent conservation. The resulting grand canonical distribution is Poissonian.

In addition to the linear behavior of the Arrhenius plots below the critical temperature, the Fisher droplet model also predicts that the cluster size distribution at the critical point must follow a power law

$$n_A(T_c) = q_0 A^{-\tau}. \tag{6}$$

If one considers clusters of both spin directions and one assumes that Eq. (4) is valid for all cluster sizes (which is not true, however not grossly incorrect), the normalization q_0 is fixed by

$$q_0 = \frac{\sum_{A=1}^{\infty} n_A(T_c)A}{\sum_{A=1}^{\infty} A^{1-\tau}}. \tag{7}$$

Away from the critical temperature, the cluster distribution should not follow a pure power law. Thus, to determine τ without a prior knowledge of the critical temperature, fits to the cluster distributions were determined for all temperatures with τ and q_0 as free parameters. At the critical temperature, the fit should have the lowest χ^2_ν and thus τ and q_0 are fixed by the fit. The best power law fit of the cluster abundances is shown in the lower panel of Fig. 3. The critical temperature was found to be $k_B T_c/J = 4.52 \pm 0.01$ with a best fit of the form $n_A(T_c) = (30\,000 \pm 5\,000) A^{(-2.30 \pm 0.08)}$. Errors are only those returned from the fitting procedure. An estimate of the systematic errors is given below. This value of the critical temperature is consistent with the value determined for infinite systems ($4.511\,52 \pm 0.000\,04 J/k_B$). The value of τ is close to the expected value for an infinite system (2.21) and is consistent with the value found by Wang (2.27) for a larger lattice [22]. The value of q_0 can be compared to Eq. (7) which yields 27566.

For the present calculations with $H_{ext}=0$ and an unconstrained magnetization, the system exists on the coexistence curve for $T<T_c$. Thus, the chemical potentials of the liquid and gas phases are equal ($\Delta\mu=0$), and Eq. (4) can be rewritten as

$$n_A(T)A^\tau/q_0 = \exp(-c_0 A^\sigma \varepsilon/T). \tag{8}$$

Therefore, a graph of the scaled cluster distributions $[n_A(T)A^\tau/q_0]$ as a function of $c_0 A^\sigma \varepsilon/T$ should collapse the distributions of all cluster sizes onto a single curve. This scaling behavior can clearly be seen in Fig. 4. This collapse below the critical temperature extends over six orders of magnitude for a broad range of cluster sizes and is very linear. Thus the clustering in the three-dimensional Ising model can be described by Fisher's droplet model. The scaling is paralleled by experimental nuclear multifragmentation data which are also shown in Fig. 4. Here the nuclear multifragmentation yields have been scaled by a factor of 100 to offset the data from the Ising cluster yields and scaled by another factor to account for the Coulomb energy present (see Refs. [9,10] for details). Agreement between Fisher's droplet model and the $d=2$ Ising model has been observed to a limited extent previously [43] although that work did not use the same cluster definition as we do.

The clusters constructed here can be properly thought of as "vapor" in equilibrium with the "liquid." Coexistence of the two phases is determined by the observation that the empirical scaling implies $\Delta\mu=0$. The fact that both the three-dimensional Ising model and the experimental nuclear multifragmentation data obey the same scaling predicted by Fisher's droplet model indicates that nuclear multifragmentation can indeed be identified as the clustering (nonideality) in a nuclear vapor in equilibrium with the nuclear liquid [4].

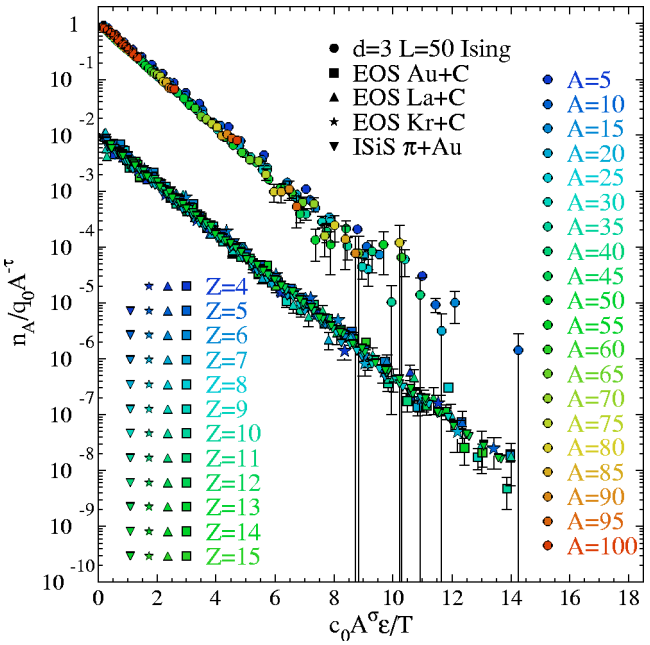

FIG. 4. (Color online) Scaling behavior of cluster distributions for the Ising model and for nuclear multifragmentation data. The nuclear multifragmentation yields have been scaled by a factor of 100 to offset the data from the Ising cluster yields and scaled by another factor to account for the Coulomb energy present, see Refs. [9,10] for details.

The quality of the scaling for the Ising model and the nuclear multifragmentation as data shown in Fig. 4 led us to test our results by simultaneously fitting the Ising cluster distributions in the Arrhenius plots using Fisher's droplet model [Eq. (5)] for temperatures up to the critical temperature. There are several methods for performing this fit. In one case, the values of τ and T_c are fixed as determined in Fig. 3 while the values of σ, c_0 , and q_0 are free. Another method allows all parameters (τ, σ, T_c, c_o, and q_0) to be determined in a single fit. The values obtained from both of these methods are consistent with those determined from the multistep method described earlier. Combining the results from all three methods allows us to estimate the errors associated with our technique giving systematic errors in σ and c_0/J of ± 0.03 and ± 1, respectively.

In order to further test the above results, we follow the method described in Refs. [9,10] and determine the magnetization based on Eq. (5). The reduced density of clusters is given by

$$\frac{\rho}{\rho_c} = \frac{\sum_A A n_A(T)}{\sum_A A n_A(T_c)} = \frac{\sum_A A^{1-\tau} \exp(-c_0 A^\sigma \varepsilon/T)}{\sum_A A^{1-\tau}} \tag{9}$$

and from this the magnetization per lattice site is simply

$$M = 1 - \frac{\rho}{\rho_c}. \tag{10}$$

Using the extracted values of σ, τ, c_0, and T_c in Eq. (9), Eq. (10) gives one branch of the magnetization curve, the

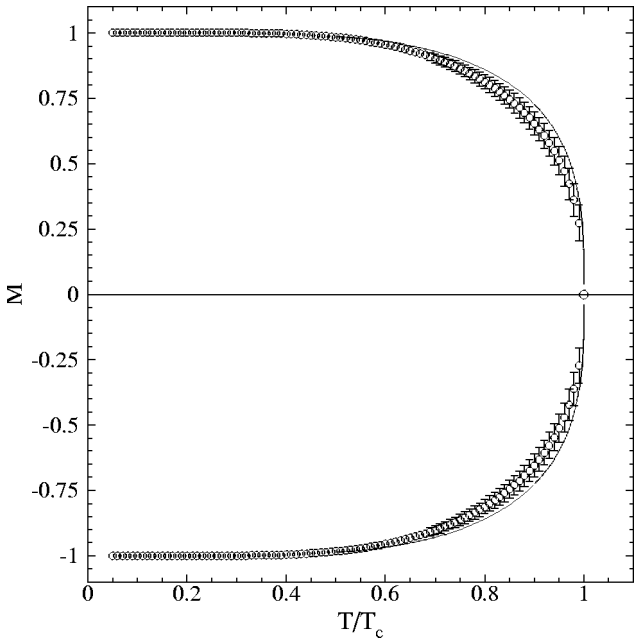

FIG. 5. The magnetization as a function of reduced temperature. The open circles show the magentization predicted via Fisher's droplet model (see text) and the solid line shows a parametrization for the magnetization.

branch for $M>0$. Since the magnetization is symmetric about the origin, the points for $M<0$ are reflections of the points for $M>0$. The results are shown as the open circles in Fig. 5. These results compare well with a parametrization for $M(T)$ [44] (used as a "benchmark") shown as a solid line in Fig. 5. Better agreement with the $M(T)$ parametrization is found when the values of $\sigma = 0.639\,46 \pm 0.0008$, $\tau = 2.209 \pm 0.006$ (from the scaling relations in Fisher's droplet model and values of $\beta = 0.326\,53 \pm 0.000\,10$ and $\gamma = 1.2373 \pm 0.002$ [44]), $c_0 = 12J$, and $T_c = 4.511\,52 \pm 0.000\,04 J/k_B$ were used. Nearly perfect results were observed when c_0 was "tuned" to 16 and the more precise value of T_c and the scaling relation exponent values were used. The agreement between the magnetization values calculated via the sum in Eq. (10) and the parametrization of Ref. [44] for $0<T<T_c$ suggests that the ideal gas assumptions in Fisher's droplet model allow for an accurate description of the system even up to densities as high as ρ_c. This contradicts results presented elsewhere [11].

In conclusion, we have shown that the clusterization in the Ising model, such as nuclear multifragmentation, portrays reducibility and thermal scaling. In addition, the Arrhenius plots allow for the extraction of barriers which are found to have a dependence of $B=c_0A^{\sigma}$, where σ is a critical exponent. The barrier coefficient from the Arrhenius plots is equivalent to the surface energy coefficient of the clusters in Fisher's droplet model. The reducibility and thermal scaling features in the Ising model can be incorporated into a Fisher-like scaling with $\Delta\mu=0$, which is obeyed over the explored temperature range below the critical temperature. Thus the observed clusters can be interpreted as a manifestation of the nonideality of a vapor in equilibrium with a liquid. Finally, nuclear multifragmentation, which is seen to share all the scaling observed here, should be similarly interpreted as characterizing the clusterization of a nuclear vapor in equilibrium with its liquid.

The authors would like to thank M. E. Fisher and D. Stauffer for their input and reviews of this paper. This work was supported by the National Science Foundation under Grant Nos. NSF-RUI 9800747 and NSF-REU 9876955 and the Nuclear Physics Division of the U.S. Department of Energy under Contract No. DE-AC03-76SF00098. One of us (C.M.M.) acknowledges support from LBNL during her sabbatical visit.

[1] L. G. Moretto *et al.*, Phys. Rep. **287**, 249 (1997).
[2] L. Beaulieu *et al.*, Phys. Rev. Lett. **81**, 770 (1998).
[3] L. G. Moretto *et al.*, Phys. Rev. C **60**, 031601 (1999).
[4] J. B. Elliott *et al.*, Phys. Rev. Lett. **85**, 1194 (2000).
[5] M. E. Fisher, Physics (Long Island City, N.Y.) **3**, 255 (1967).
[6] M. E. Fisher, Rep. Prog. Phys. **30**, 615 (1969).
[7] C. S. Kiang and D. Stauffer, Z. Phys. **235**, 130 (1970).
[8] D. Stauffer and C. S. Kiang, Adv. Colloid Interface Sci. **7**, 103 (1977).
[9] J. B. Elliott *et al.*, Phys. Rev. Lett. **88**, 042701 (2002).
[10] J. B. Elliott *et al.*, Phys. Rev. C **67**, 024609 (2003).
[11] F. Gulminelli *et al.*, Phys. Rev. C **65**, R051601 (2002).
[12] D. Stauffer, Phys. Rep. **54**, 2 (1979).
[13] D. Stauffer and A. Aharony, *Introduction to Percolation Theory*, 2nd ed. (Taylor and Francis, London, 1992).
[14] W. Bauer *et al.*, Phys. Lett. **150B**, 53 (1985).
[15] W. Bauer *et al.*, Prog. Part. Nucl. Phys. **99**, 42 (1999).
[16] P. D. Gujrati, Phys. Rev. E **51**, 957 (1995).
[17] D. Stauffer, Phys. Rev. Lett. **35**, 394 (1975).
[18] C. Domb and E. Stoll, J. Phys. A **10**, 1141 (1977).
[19] A. Coniglio and W. Klein, J. Phys. A **13**, 2775 (1980).
[20] J. L. Cambier and M. Nauenberg, Phys. Rev. B **34**, 8071 (1986).
[21] J. Kertész, Physica A **161**, 58 (1989).
[22] J. S. Wang, Physica A **161**, 249 (1989).
[23] J. S. Wang and R. H. Swendsen, Physica A **167**, 565 (1990).
[24] D. De Meo, D. W. Heermann, and K. Binder, J. Stat. Phys. **60**, 585 (1990).
[25] A. M. Ferrenberg and D. P. Landau, Phys. Rev. B **44**, 5081 (1991).
[26] J. J. Alonso, A. I. López-Lacomba and J. Marro, Phys. Rev. E **52**, 6006 (1995).
[27] S. K. Samaddar and J. Richert, Phys. Lett. B **218**, 381 (1989).
[28] S. K. Samaddar and J. Richert, Z. Phys. A **332**, 443 (1989).
[29] J. Pan and S. Das Gupta, Phys. Lett. B **344**, 29 (1995).
[30] J. Pan and S. Das Gupta, Phys. Rev. C **51**, 1384 (1995).

[31] S. Das Gupta and J. Pan, Phys. Rev. C **53**, 1319 (1996).
[32] X. Campi and H. Krivine, Nucl. Phys. **A620**, 46 (1997).
[33] F. Gulminelli and Ph. Chomaz, Phys. Rev. Lett. **82**, 1402 (1999).
[34] Ph. Chomaz and F. Gulminelli, Phys. Lett. B **447**, 221 (1999).
[35] F. Gulminelli and Ph. Chomaz, Phys. Rev. Lett. **82**, 1402 (1999).
[36] V. Duflot, Ph. Chomaz, and F. Gulminelli, Phys. Lett. B **476**, 279 (2000).
[37] X. Campi, H. Krivine, and A. Puente, Physica A **262**, 328 (1999).
[38] P. Butera and M. Comi, Phys. Rev. B **65**, 144431 (2002).
[39] T. D. Lee and C. N. Yang, Phys. Rev. **87**, 404 (1952).
[40] T. D. Lee and C. N. Yang, Phys. Rev. **87**, 410 (1952).
[41] H. Gould and J. Tobochnik, *An Introduction to Computer Simulation Methods–Applications to Physical Systems*, 2nd ed. (Addison-Wesley, Reading, MA, 1996).
[42] D. Stauffer, Int. J. Mod. Phys. C **10**, 809 (1999).
[43] E. Stoll *et al.*, Phys. Rev. B **6**, 2777 (1972).
[44] K. Okunishi and T. Nishino, Prog. Theor. Phys. **103**, 541 (2000).